The Azulene S_1 State Decays via a Conical Intersection: A CASSCF Study with MMVB Dynamics

Michael J. Bearpark,[†] Fernando Bernardi,[‡] Simon Clifford,[†] Massimo Olivucci,*[,‡] Michael A. Robb,*[,†] Barry R. Smith,[†] and Thom Vreven[†]

Contribution from the Dipartimento di Chimica "G. Ciamician" dell' Universitá di Bologna, Via Selmi 2, 40126 Bologna, Italy, and Department of Chemistry, King's College London, Strand, London WC2R 2LS, U.K.

Received May 5, 1995[⊗]

Abstract: The anomalous fluorescence of azulene—emission from S_2 rather than S_1—was first recognized by Beer and Longuet-Higgins 40 years ago. Femtosecond laser studies and spectroscopic line width measurements have now established that radiationless decay from S_1 to the ground state takes place in less than 1 ps. In this paper we show how such ultrafast S_1 decay can be explained by relaxation through an unavoided S_1/S_0 crossing (i.e., a conical intersection). The S_1 relaxation dynamics of azulene from its Franck−Condon structure are modeled semiclassically using a hybrid quantum-mechanical/force-field potential (MMVB) which reproduces the structure of the *ab initio* CASSCF potential energy surface. This simulation suggests that *the $S_1 \rightarrow S_0$ decay takes place in femtoseconds before a single oscillation through the crossing is completed.*

Introduction

The anomalous fluorescence of azulene—emission from S_2 rather than S_1—was first recognized by Beer and Longuet-Higgins 40 years ago[1] and has been studied continuously ever since.[2−6] However, Longuet-Higgins' original suggestion that an intersection of the S_0 and S_1 potential energy surfaces would lead to fast internal conversion (IC) rather than fluorescence has never been accepted. (For instance, it was argued[2a] that, since $\Delta E(S_0-S_1)$ and $\Delta E(S_1-S_2)$ were both ∼14 000 cm^{-1}, IC should be equally unlikely in either case.) However, Hunt and Ross[3] observed that vibrational lines in the S_1 absorption spectrum of azulene vapor were much more diffuse (∼10−20 cm^{-1}) than those of the higher-energy S_2 spectrum (∼1 cm^{-1}), which required that the S_1 lifetime be shorter and <100 ps. They suggested that a decrease in the azulene transannular bond length on excitation to S_1 could close the S_0-S_1 energy gap and lead to IC via tunneling. Rentzepis[4a−f] measured the S_1 lifetime directly (7.5 ps in solution[4b]) and finally detected extremely weak fluorescence from S_1 with $\Phi_f \sim 10^{-6}$ [4b] (comparable with $S_2 \rightarrow S_1$ fluorescence.)[7]

This very short nonradiative decay time has now been confirmed by many subsequent spectroscopic studies using both picosecond[4g−k] and femtosecond[6] pulsed lasers and spectral line widths.[5a, d−g] The dependence of the azulene S_1 lifetime on heavy atom solvent, deuteration, and vibrational excess energy has also been investigated. Ippen and Schank *et al.*[4j] found that complete deactivation of the azulene S_1 state took place in 1.9 ± 0.2 ps, unaffected by heavy atom solvent or deuteration. Since the ground state repopulation time was the same as the S_1 decay time,[4k] Ippen and Schank concluded that vibrational relaxation within S_1 was fast in solution compared to IC. However, in the solid state (azulene-in-naphthalene crystals at <4.2 K), IC and vibrational relaxation were found to be competitive[5b,c] and deuteration decreased the line width in the S_1 emission by ∼25%.[5a] Kulkarni and Kenny[5f] found a strong excess energy dependence of the S_1 lifetime in a jet experiment which halved from ∼1 to ∼0.5 ps with an excess energy of 1000 cm^{-1}. Because the lifetimes determined from absorption line widths in jet experiments (∼1 ps)[5d−f] were less than those determined by pulsed lasers in solution (∼2 ps),[4a−k] Schwartzer, Troe, and Schroeder,[6a] and Wagner and Steer[6b] repeated the solution measurements with femtosecond resolution. Both obtained a value of 1.0 ± 0.1 ps and agreed that this value was independent of deuteration or heavy atom solvent. Although it has recently been reported[5g] that the azulene S_1 lifetime in viscous ethylene glycol solution may increase to 3.0 ps, Wagner

[†] Universitá di Bolongna.

[‡] King's College London.

[⊗] Abstract published in *Advance ACS Abstracts,* December 15, 1995.

(1) Beer, M.; Longuet-Higgins, H. C. *J. Chem. Phys.* **1955**, *23*, 1390−1391.

(2) (a) Viswanath, G.; Kasha, M. *J. Chem. Phys.* **1956**, *24*, 574−577. (b) Sidman, J. W.; McClure, D. S. *J. Chem. Phys.* **1956**, *24*, 757−763.

(3) (a) Hunt, G. R.; Ross, I. G. *J. Mol. Spectrosc.* **1962**, *9*, 50−78. (b) McCoy, E. F.; Ross, I. G. *Aust. J. Chem.* **1962**, *18*, 573−590. (c) Hunt, G. R.; McCoy, E. F.; Ross, I. G. *Aust. J. Chem.* **1962**, *18*, 591−604.

(4) (a) Rentzepis, P. M. *Chem. Phys. Lett.* **1968**, *2*, 117. (b) Rentzepis, P. M. *Chem. Phys. Lett.* **1969**, *3*, 717−720. (c) Rentzepis, P. M. *Photochem. Photobiol.* **1968**, *8*, 579. (d) Rentzepis, P. M. *Chem. Phys. Lett.* **1971**, *10*, 193. (e) 4833. (f) Huppert, D.; Rentzepis, P. M. In *Molecular Energy Transfer*; Levine, R., Jortner, J., Eds.; Wiley: New York, 1976; pp 275−279. (g) Drent, E.; Makkes van der Deijl, G. Zandstra, P. *Chem. Phys. Lett.* **1968**, *2*, 526−528. (h) Wirth, P.; Schneider, S.; Dörr, F. *Chem. Phys. Lett.* **1976**, *42*, 482−487. (i) Heritage, J. P.; Penzkofer, A. *Chem. Phys. Lett.* **1976**, *44*, 76−81. (j) Ippen, E. P.; Shank, C. V.; Woerner, R. L. *Chem. Phys. Lett.* **1977**, *46*, 20−23. (k) Shank, C. V.; Ippen, E. P.; Teschke, O.; Fork, R. L. *Chem. Phys. Lett.* **1978**, *57*, 433.

(5) (a) Hochstrasser, R. M.; Li, T.-Y. *J. Mol. Spectrosc.* **1972**, *41*, 297−301. (b) Friedman, J. M.; Hochstrasser, R. M. *Chem. Phys.* **1974**, *6*, 145−154. (c) Hochstrasser, R. M.; Nyi, C. A. *J. Chem. Phys.* **1979**, *70*, 1112−1128. (d) Amirav, A.; Jortner, J. *J. Chem. Phys.* **1984**, *81*, 4200−4205. (e) Suzuki, T.; Ito, M. *J. Phys. Chem.* **1987**, *91*, 3537−3542. (f) Kulkarni, S. K.; Kenny, J. E. *J. Chem. Phys.* **1988**, *89*, 4441−4442. (g) Matsumoto, T.; Ueda, K.; Tomita, M. *Chem. Phys. Lett.* **1992**, *191*, 627−632.

(6) (a) Schwarzer, D.; Troe, J.; Schroeder, J. *Ber. Bunsen-Ges. Phys. Chem.* **1991**, *95*, 933−934. (b) Wagner, B. D.; Szymanski, M.; Steer, R. P. *J. Chem. Phys.* **1993**, *98*, 301−307. (c) Tittelbach-Helmrich, D.; Wagner, B. D.; Steer, R. P. *Chem. Phys. Lett.* **1993**, *209*, 464−468. (d) Tittelbach-Helmrich, D.; Wagner, B. D.; Steer, R. P. *Can. J. Chem.* **1995**, *73*, 303−306. (e) Tittelbach-Helmrich, D.; Steer, R. P. *Chem. Phys.* **1995**, *197*, 99−106.

(7) (a) Rentzepis, P. M.; Jortner, J.; Jones, R. P. *Chem. Phys. Lett.* **1970**, *4*, 599−602. (b) Huppert, D.; Jortner, J.; Rentzepis, P. M. *Chem. Phys. Lett.* **1972**, *13*, 225−228. (c) Gillispie, G. D.; Lim, E. C. *J. Chem. Phys.* **1976**, *65*, 4314. (d) Gillispie, G. D.; Lim, E. C. *J. Chem. Phys.* **1978**, *68*, 4578−4586. (e) Klemp, D.; Nickel, B. *Chem. Phys. Lett.* **1986**, *130*, 493−497. (f) Wagner, B. D.; Tittelbach-Helmrich, D.; Steer, R. P. *J. Phys. Chem.* **1992**, *96*, 7904−7908.

0002-7863/96/1518-0169$12.00/0

and Steer[6c] were not able to reproduce this effect. They did find that the lifetime increased in a more polar solvent but suggested that this was well-correlated with the energy gap between S_0 and S_1 in the different media and not connected with the structure of the solvent itself.

Although the lifetime of the S_1 state of azulene is now accepted to be less than 1 ps, the origin of this observation has remained a mystery[6b] despite Longuet-Higgins' original suggestion that a state crossing was involved. In this paper, we demonstrate (by gradient-directed optimization) the existence of an unavoided S_0/S_1 crossing (i.e., a conical intersection) located a few kcal mol^{-1} above the azulene S_1 minimum. This conical intersection is the lowest energy point on a 46-dimensional hyperline (a subspace of 48 nuclear coordinates) where the S_1 and S_0 states cross. The radiationless decay process at the crossing is investigated by simulating relaxation from the Franck−Condon region using a hybrid quantum-mechanical/force-field potential. This simulation suggests that *decay can take place before a single S_1 oscillation is completed* and that return to the ground state is therefore expected to occur on the femtosecond time scale, independent of S_1 vibrational cooling or equilibration.

Computational Details

Our goal in this work is to model the radiationless decay dynamics of azulene via a conical intersection. Dynamics computations are still too expensive to be carried out using *ab initio* methods on molecules of this size. Our semiclassical dynamics method (see ref 8a for details) uses a hybrid quantum-mechanical/force-field potential (MMVB[8b]) designed to reproduce the results of *ab initio* CASSCF computations. To establish that this nonequilibrium simulation will correctly describe the decay process, we have characterized the relevant critical points on the azulene S_0 and S_1 potential energy surfaces using CASSCF[9] and CASSCF+GVB,[10] demonstrating that the MMVB surface has the correct structural features.

Ab Initio Computations. The most critical feature of a CASSCF calculation is the choice of active space. The obvious choice for describing the S_1 state of azulene would be 10 electrons in 10 π molecular orbitals (MOs), which we refer to as CAS10 here. Computations with such large active spaces are expensive if used for the complete documentation of a potential energy surface because of the size of the eigenvalue problem and the time taken to compute the gradient in conical intersection optimizations. However, in the region of the S_0 and S_1 minima and the S_0/S_1 crossing, we can truncate the 10π active space to 6π (CAS6) because two of the 10 π MOs are almost doubly occupied (>1.9) and two are almost unoccupied (<0.1).

Because the S_1 excited state of azulene is covalent (having a small measured dipole moment of 0.42D,[11]) a 4-31G basis set was used for CAS6 and CAS10 calculations. (CAS6 is equivalent to CAS6/4-31G and CAS10 equivalent to CAS10/4-31G throughout the rest of the paper.) Roos[12] has previously shown that large basis sets and diffuse functions are not essential for the correct CASSCF description of excited states of conjugated hydrocarbons unless the state in question has ionic or Rydberg character. However, in order to confirm the crucial topology and energetics, we have reoptimized two structures—the S_1 minimum and the S_0/S_1 conical intersection—using the 6-31G* basis set and the CASSCF+GVB[10] method. In this method, each of the 175 CAS6 configurations is augmented with two GVB pair excitations (CAS6 + GVB). In the S_0/S_1 crossing region, the GVB pair orbitals can be localized as double bonds in the seven-membered ring whose only function is to include part of the dynamic correlation energy. Because of the nature of the GVB configurations, the gradient computation is much faster than a full CAS10 gradient.

Conical intersections[13] have been extensively discussed in the literature,[14] and recent investigations have indicated that they can be a common feature in organic systems.[15] A conical intersection is an $n - 2$ dimensional subspace of the n nuclear coordinates called intersection space. The energy of the two states remains the same at any point in this space; the degeneracy is only lifted when the molecule is distorted along the two remaining linearly-independent nuclear coordinates x_1 and x_2, the nonadiabatic coupling and gradient difference vectors. The nonstandard method[16] used to locate minimum energy points in the $n - 2$ dimensional intersection space has been implemented in a development version of Gaussian 92.[9]

The full optimization of the conical intersection was carried out using the CAS6/4-31G and CAS6+GVB/6-31G* methods. Although the azulene conical intersection minimum has C_{2v} symmetry,[17] the intersection is not restricted to C_{2v} geometries. As we shall show with the decay simulation, S_1/S_0 crossing can take place at a range of lower-symmetry geometries in the region of the intersection minimum.

MMVB Dynamics. The MMVB hybrid method[8b] uses the molecular mechanics MM2 force field[19] to describe the inert molecular σ-framework and a parametrized Heisenberg Hamiltonian[20] to simulate the CASSCF active orbitals in a valence bond space. Because of the nature of the Heisenberg Hamiltonian, MMVB has the ability to reproduce the CASSCF potential energy surface for *covalent* electronic states (see for example ref 18). A general set of molecular VB parameters (which simulate CASSCF/4-31G* energies) is available for a sp^2/sp^3 carbon at present.[8b] MMVB has already been tested for a 10 active electron system, reproducing[21] the CASSCF geometries obtained

(8) (a) Bearpark, M. J.; Robb, M. A.; Smith, B. R.; Bernardi, F.; Olivucci, M. *Chem. Phys. Lett.* **1995**, *242*, 27−32. (b) Bernardi, F.; Olivucci, M.; Robb, M. A. *J. Am. Chem. Soc.* **1992**, *114*, 1606−1616.

(9) Frisch, M. J.; Trucks, G. W.; Head-Gordon, M.; Gill, P. M. W.; Wong, M. W.; Foresman, J. B.; Schlegel, H. B.; Robb, M. A.; Reploge, E. S.; Gomperts, R.; Andres, J. L.; Raghavachari, K.; Binkley, J. S.; Gonzales, C.; Martin, R. L.; Fox, D. J.; Defrees, D. J.; Baker, J.; Stewart, J. J. P.; Pople, J. A. *Gaussian 92, Revision B*; Gaussian, Inc.: Pittsburgh, PA, 1992.

(10) Goddard, W. A.; Harding, L. B. *Annu. Rev. Phys. Chem.* **1978**, *29*, 363.

(11) (a) Hochstrasser, R. M.; Noe, L. J. *J. Chem. Phys.* **1969**, *50*, 1684−1688. (b) Barker, J. W.; Noe, L. J.; Marchetti, A. P. *J. Chem. Phys.* **1973**, *59*, 1304−1313.

(12) Serrano-Andrés, L.; Merchan, M.; Nebot-Gil, I.; Lindh, R.; Roos, B. O. *J. Chem. Phys.* **1993**, *98*, 3151−3162.

(13) Salem, L. *Electrons in Chemical Reactions: First Principles*; Wiley: New York, 1982.

(14) (a) Von Neumann, J.; Wigner, E. *Phys. Z.* **1929**, *30*, 467. (b) Teller, E. *J. Phys. Chem.* **1937**, *41*, 109. (c) Kauzmann, W. *Quantum Chemistry*; Academic Press: New York, 1957; pp 696−697. (d) Barrow, G. M. *Introduction to Molecular Spectroscopy*; McGraw-Hill: New York, 1962; pp 306. (e) Herzberg, G.; Longuett-Higgins, H. C. *Trans. Faraday Soc.* **1963**, *35*, 77. (f) Herzberg, G. *The Electronic Spectra of Polyatomic Molecules*; Van Nostrand: Princeton, 1966; pp 442. (g) Teller, E. *Israel J. Chem.* **1969**, *7*, 227. (h) Gerhartz, W.; Poshusta, R. D.; Michl, J. *J. Am. Chem. Soc.* **1977**, *99*, 4263. (i) Michl, J.; Bonacic-Koutecky, V. *Electronic Aspects of Organic Photochemistry*; Wiley: New York, 1990. (j) Bonacic-Koutecky, V.; Koutecky, J.; Michl, J. *Angew. Chem., Int. Ed. Engl.* **1987**, *26*, 70. (k) Mead, C. A.; Truhlar, D. G. *J. Chem. Phys.* **1979**, *70*, 2284. (l) Keating, S. P.; Mead, C. A. *J. Chem. Phys.* **1987**, *86*, 2152. (m) Tully, J. C.; Preston, R. K. *J. Chem. Phys.* **1987**, *55*, 562. (n) Blais, N. C.; Truhlar, D. G.; Mead, C. A. *J. Chem. Phys.* **1988**, *89*, 6204.

(15) (a) Bernardi, F.; De, S.; Olivucci, M.; Robb, M. A. *J. Am. Chem. Soc.* **1990**, *112*, 1737. (b) Palmer, I. J.; Ragazos, I. N.; Bernardi, F.; Olivucci, M.; Robb, M. A. *J. Am. Chem. Soc.* **1993**, *115*, 673−682. (c) Olivucci, M.; Ragazos, I. N.; Bernardi, F.; Robb, M. A. *J. Am. Chem. Soc.* **1993**, *115*, 3710−3721. (d) Olivucci, M.; Bernardi, F.; Celani, P.; Ragazos, I. N.; Robb, M. A. *J. Am. Chem. Soc.* **1994**, *116*, 1077−1085. (e) Celani, P.; Ottani, S.; Olivucci, M.; Bernardi, F.; Robb, M. A. *J. Am. Chem. Soc.* **1994**, *116*, 10141−10151. (f) Yamamoto, N.; Bernardi, F.; Bottoni, A.; Olivucci, M.; Robb, M. A.; Wilsey, S. *J. Am. Chem. Soc.* **1994**, *116*, 2064. (g) Bearpark, M. J.; Olivucci, M.; Wilsey, S.; Bernardi, F.; Robb, M. A. *J. Am. Chem. Soc.* **1995**, *117*, 6944−6953. (h) Bernardi, F.; Olivucci, M.; Robb M. A. *Israel. J. Chem.* **1993**, *33*, 265−276.

(16) (a) Ragazos, I. N.; Robb, M. A.; Bernardi, F.; Olivucci, M. *Chem. Phys. Lett.* **1992**, *197*, 217. (b) Bearpark, M. J.; Robb, M. A.; Schlegel, H. B. *Chem. Phys. Lett.* **1994**, *223*, 269−274.

(17) (a) Longuett-Higgins, H. C. *Proc. R. Soc. London, Ser. A* **1975**, *344*, 147. (b) Stone, A. J. *J. Chem. Soc., Faraday Trans.* **1994**, *90*, 1673.

(18) Bernardi, F.; Ragazos, I. N.; Olivucci, M.; Robb, M. A. *J. Am. Chem. Soc.* **1992**, *114*, 8211−8220.

(19) Allinger, N. L. *Adv. Phys. Org. Chem.* **1976**, *13*, 1.

(20) (a) Anderson, P. W. *Phys. Rev.* **1959**, *115*, 2. (b) Said, M.; Maynau, D.; Malrieu, J.-P.; Bach, M.-A. G. *J. Am. Chem. Soc.* **1984**, *106*, 571−579. (c) Said, M.; Maynau, D.; Malrieu, J.-P. *J. Am. Chem. Soc.* **1984**, *106*, 580−587. (d) Durand, P.; Malrieu, J.-P. *Adv. Chem. Phys.* **1987**, *67*, 321−412.

(21) Bearpark, M. J.; Bernardi, F.; Olivucci, M.; Robb, M. A. *Chem. Phys. Lett.* **1994**, *217*, 513−519.

for the S_0 and S_1 states of naphthalene by Dupuis et al.[22] As we shall discuss subsequently, the MMVB geometries and potential energy surface structure of azulene are in good agreement with the corresponding CASSCF results.

The MMVB energy and gradient are used to solve the equations of motion for azulene.[23] Full details of our implementation have been given.[8a] The trajectories are propagated using a series of local quadratic approximations to the MMVB potential energy surface, as suggested by Helgaker et al.[24] The step size is determined by a trust radius.[25] Initial conditions (i.e., the initial velocities) are determined by random sampling of each excited state normal mode within an energy threshold ΔE_{limit}, starting at the Franck−Condon geometry (S_0*) on S_1. This generates an ensemble of trajectories—a "classical wave packet". For each value of ΔE_{limit}, 256 trajectories were run, each for several hundred steps. The surface-hopping algorithm of Tully and Preston[23] is used to allow excited state trajectories to transfer to the ground state in the conical intersection region, where strong nonadiabatic coupling effects appear. The difference in energy between S_0 and S_1 at the hop is then redistributed along the component of the momentum parallel to the nonadiabatic coupling vector, as described by Truhlar.[14n]

Loss of kinetic energy due to solvent interactions has not been included in our simulation (although a simple Stoke's Law viscosity model has been implemented). This is because, experimentally, the decay does not seem to be affected by vibrational relaxation (i.e., equilibration) on S_1. The anomalous fluorescence of azulene is observed in the gas phase[4e] (both with and without an inert bath gas) as well as in liquid and solid solutions, which suggests that the same mechanism operates irrespective of the detailed structure of the medium.[5d,e,6b]

Results and Discussion

In Figure 1 we outline the surface topology in the region of the S_1 minimum computed with CAS6 and MMVB. Energies computed at all levels of theory are collected in Tables 1 and 2, and the CAS10 and CAS6+GVB/6-31G* geometries are shown in Figure 2. We concentrate first on the surface topology, discussing the dynamics results in the next section.

Surface Topology and Energetics. Figure 1 shows that the CAS6 and MMVB S_1 surface topologies are the same: a minimum located between the Franck−Condon geometry (S_0*) and an S_1/S_0 sloped[26] conical intersection. The existence of a conical intersection would explain the observed lack of fluorescence from S_1 if the difference in energy between the S_1 minimum and the lowest energy intersection point is sufficiently small, as IC may then approach 100% efficiency. However, this energy difference (unlike the surface topology itself) is sensitive to the method of computation. The MMVB value is ∼1 kcal mol^{-1} (Figure 1). Using CAS6 it increases to ∼13 kcal mol^{-1}, decreasing with the more accurate CAS6+GVB/6-31G* to 7.3 kcal mol^{-1}. While the barrier height has not been calculated to chemical accuracy here, both the *ab initio* and MMVB results establish that *the geometrical distortion connecting the Franck−Condon structure to the optimized S_1 minimum also connects the minimum to the crossing point* (Scheme 1, top of Figure 1). This feature of the S_1 surface plus simple inertia arguments suggest that an azulene molecule relaxing from the Franck−Condon structure will cross to S_0 *before* a single oscillation through the S_1 surface well is completed (arrows in Figure 1). One therefore expects that the energy threshold to the crossing point is unimportant and that the only restriction to decay is that the Franck−Condon structure must lie energetically above the intersection point.

In order to establish that our computations provide a qualitatively correct description of the S_1 relaxation dynamics, we now discuss a few essential results in more detail. These

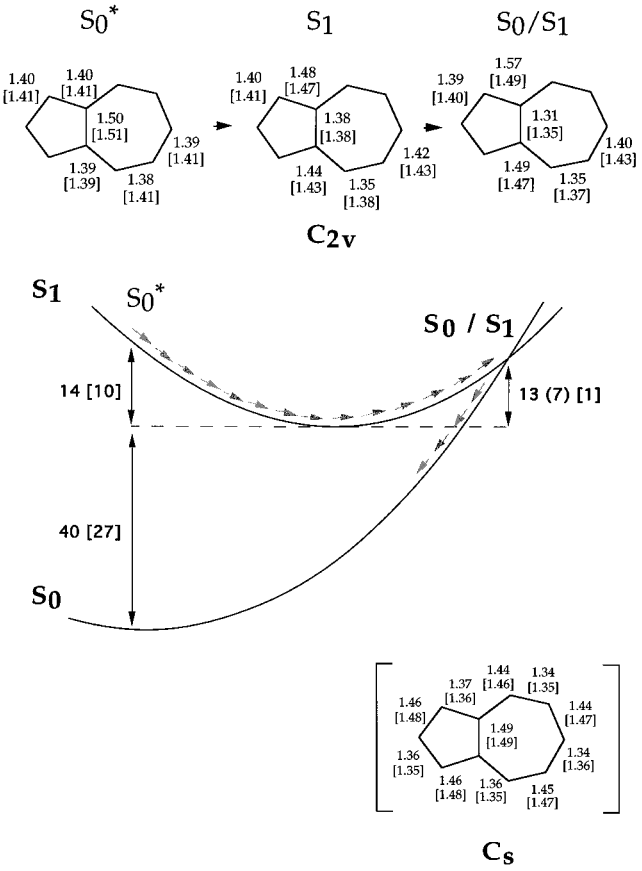

Figure 1. CAS6/4-31G and MMVB (square brackets) energies (kcal mol^{-1}) and geometries (Å) of the C_{2v} critical points on the S_0 and S_1 potential energy surfaces of azulene. The C_s bond-alternating S_0 structure—discussed in the text—is shown bottom right. The CAS6+GVB/6-31G* energy difference between the S_0 minimum and S_0/S_1 crossing is shown in parentheses.

Table 1. CAS6/4-31G Energies/at 4-31G Optimized Geometries

geometry	Figure	S_0/E$_h$	S_1/E$_h$	E (kcal mol^{-1})
S_0 C_s	1	−382.8085	−382.6931	72
S_0 C_{2v}	1	−382.7999	−382.7124	55
S_1	1	−382.7739	−382.7354	24
		−382.7699[a]	−382.7303[a]	25
S_0/S_1	1	−382.7104[a]	−382.7091[a]	<1

[a] State-averaged orbitals.

Table 2. CAS10/4-31G Energies at 4-31G Optimized Geometries

geometry	Figure	S_0	S_1	ΔE (kcal mol^{-1})
S_0 C_s	2	−382.8737	−382.7934	50
S_0 C_{2v}	2	−382.8733	−382.8014	45
S_1	2	−382.8550	−382.8155	25
		−382.8530[a]	−382.8141[a]	24
S_0/S_1 (CAS6)	1	−382.7817[b]	−382.7812[b]	<1
		−382.7886[a]	−382.7861[a]	<2
S_0/S_1[c]	2	−382.7967[a]	−382.7954[a]	<1
S_0/S_1 (MMVB)	1	−382.8216[a]	−382.7995[a]	14

[a] State-averaged orbitals. [b] CAS10 configuration interaction only, using optimized CAS6 state-averaged orbitals. [c] Partially reoptimized (two steps) CAS6 geometry. Forces not converged.

(22) Swiderek, P.; Hohlneicher, G.; Maluendes, S. A.; Dupuis, M. *J. Chem. Phys.* **1993**, *98*, 975. The napthalene experimental S_1 geometry was obtained by calculating changes relative to the ground state from Franck−Condon factors: Innes, K. K. In *Excited States*; Lim, E. C., Ed.; Academic Press: New York, 1975; Vol. 2.

(23) (a) Preston, R. K.; Tully, J. C. *J. Chem. Phys.* **1971**, *54*, 4297. (b) Preston, R. K.; Tully, J. C. *J. Chem. Phys.* **1971**, *55*, 562.

(24) Helgaker, T.; Uggerud, E.; Jensen, H. J. A. *Chem. Phys. Lett.* **1990**, *173*, 145−150.

(25) Chen, W.; Hase, W. L.; Schlegel, H. B. *Chem. Phys. Lett.* **1994**, *228*, 436−442.

(26) Atchity, G. J.; Xantheas, S. S.; Ruedenberg, K. *J. Chem. Phys.* **1991**, *95*, 1862−1876.

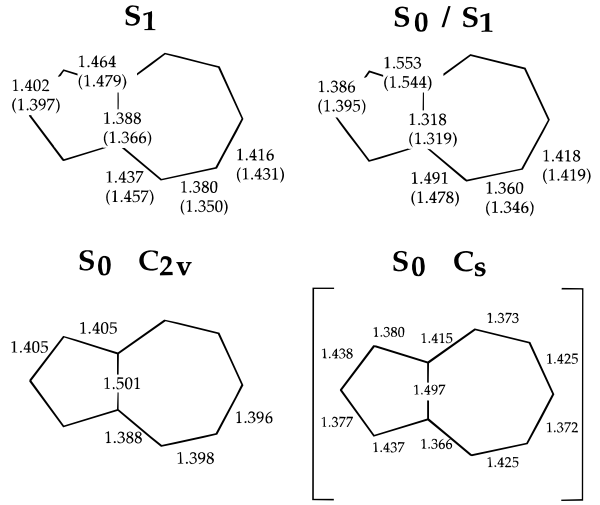

Figure 2. CAS10/4-31G geometries (Å) of the C_{2v} critical points on the S_0 and S_1 potential energy surfaces of azulene (bottom and top left, respectively), C_s bond-alternating S_0 structure (bottom right), and S_0/S_1 surface crossing (top right). The CAS6+GVB/6-31G* bond lengths are shown in brackets.

include (i) the Franck−Condon structure (S_0*), (ii) the S_1 minimum structure and S_1 energetics, and (iii) the relaxation coordinate.

(i) The Franck−Condon Structure (S_0*). There is some experimental evidence to suggest that azulene is very flexible in the antisymmetric ground state coordinate which leads to the C_s structures with alternate single and double bonds shown bottom right in Figures 1 and 2. Both Hochstrasser and Nyi[5c] and Small and Kusserow[27] observed b_2 modes in the excitation spectrum, as well as progressions in the totally symmetric a_1 modes. The crystal structure is disordered.[28ab]

Recent UNO-CAS/6-31G* calculations by Pulay[29m] locate a C_{2v} transition structure only 32 cm^{-1} above the C_s minima, which disagrees with the B3-LYP/6-31G* density functional prediction of a C_{2v} minimum. The fact that scaled B3-LYP/6-31G* frequencies best reproduce the oriented crystal IR spectrum[27e] favors a C_{2v} structure for the S_0 minimum. In this work (CAS10) we found the S_0 C_s and C_{2v} structures (Figure 2) to be <1 kcal mol^{-1} apart (Table 2) in agreement with Pulay.[29m] MMVB and CAS6 exaggerate this energy difference (∼6 kcal mol^{-1}, Table 1), but since the most accurate computations[29j−m] suggest that the C_{2v} structure is a shallow minimum, we have used it as the starting point (S_0*) for the S_1 dynamics computations with MMVB.

(ii) The S_1 Minimum Structure and S_1 Energetics. The most important geometric change occurring on exciting azulene to S_1 is the contraction (1.50 to 1.39 Å) of the transannular bond (Figures 1 and 2, Scheme 1). An "experimental" geometry for the S_1 equilibrium structure of azulene was previously obtained by Zerbetto and Zgierski[29h] using the QCFF/PI normal modes for S_0 together with displacement parameters calculated from the resonance Raman spectra of Page et al.[30] The CASSCF S_1 geometry obtained by Negri and Zgierski is very close to our CAS10 geometry (all bond lengths are within 0.01 Å, Figure 2); this geometry hardly changes at the MMVB or CAS6 levels (Figure 1) and is very close to the "experimental" one.[29h] Both QCFF/PI alone and CIS underestimated[29h,k] the changes in the transannular and adjacent C−C bonds on excitation.

Scheme 1

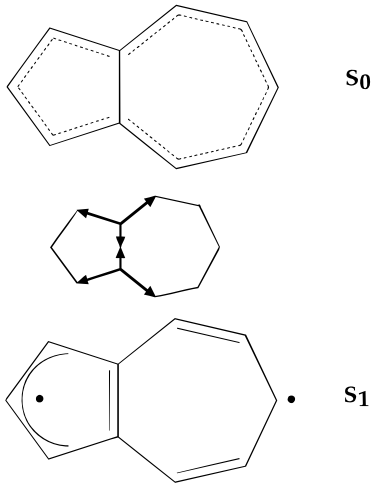

The energy differences between the Franck−Condon geometry, the S_1 minimum, and the S_1/S_0 conical intersection control the kinetic energy available in the surface hop region in the dynamics computations. Energies for the 0−0 transition can be compared with the experimental value of 40.7 kcal mol^{-1}.[5d] The CAS10 value is 36 kcal mol^{-1} (Table 2), and the CAS6 value 40 kcal mol^{-1} (Table 1). MMVB gives only 27 kcal mol^{-1}. Since azulene S_0 is easily distorted along the antisymmetric b_2 coordinate in its ground state, we have also calculated vertical excitation energies at the C_s geometries. Using CAS10 (Table 2), this is ∼50 kcal mol^{-1} and the CAS6 value (Table 1) is 72 kcal mol^{-1} (which is over 30 kcal mol^{-1} greater than the 0−0 energy). Both values suggest that the antisymmetric coordinate in the excited state is much stiffer and that there is a deep channel leading to the C_{2v} minimum on S_1.

(iii) The Relaxation Coordinate. The relaxation coordinate linking the Franck−Condon geometry with the S_1 minimum in C_{2v} symmetry is illustrated in Figure 1 (top) and Scheme 1. This coordinate involves compression of the transannular bond (described above) together with expansion of the adjacent C−C bonds within the ring (Figures 1 and 2). At the S_1 minimum, the S_0-S_1 energy gap is ∼25 kcal mol^{-1}, approximately one-half that at the Franck−Condon geometry (Tables 1 and 2). Following this coordinate through the S_1 minimum, the gap continues to shrink, leading ultimately to a conical intersection. Using CAS6, the S_0/S_1 conical intersection is located ∼13 kcal mol^{-1} above the S_1 minimum, compared to ∼1 kcal mol^{-1} for MMVB. In order to confirm the nature of the surface topology, the geometries of the S_1/S_0 conical intersection and the S_1 minimum were reoptimized using the CAS6+GVB/6-31G* method described above. The reoptimized geometries are shown

(27) Small, G. J.; Kusserow, S. *J. Chem. Phys.* **1974**, *60*, 1558−1563.
(28) (a) Monteath Robertson, J.; Shearer, H. M. M.; Sim, G. A.; Watson, D. G. *Acta Crystallogr.* **1962**, *15*, 1. (b) Hanson, A. W.; *Acta Crystallogr.* **1965**, *19*,19. (c) Bastiansen, O.; Derrisen, J. L. *Acta Chem. Scand.* **1966**, *20*, 1319−1324. (d) Dorko, E. A.; Hencher, J. L.; Bauer, S. H. *Tetrahedron* **1968**, *24*, 2475. (e) Bree, A.; Pal, A. J.; Taliani, C. *Spectrochim. Acta A* **1990**, *47*, 1767−1778.
(29) (a) Pariser, R. *J. Chem. Phys.* **1956**, *25*, 1112. (b) Bloor, J. E. *Can. J. Chem.* **1965**, *43*, 3026. (c) Buenker, R. J.; Peyerimhoff, S. D. *Chem. Phys. Lett.* **1969**, *3*, 37. (d) Gerhartz, W.; Michl, J. *J. Am. Chem. Soc.* **1978**, *100*, 6877. (e) Kollmar, H. *J. Am. Chem. Soc.* **1979**, *101*, 4832. (f) Haddon, R. C.; Raghavachari, K. *J. Am. Chem. Soc.* **1982**, *104*, 3516. (g) Glidewell, C.; Lloyd, D. *Tetrahedron* **1984**, *40*, 4455. (h) Zerbetto, F.; Zgierski, M. Z. *Chem. Phys.* **1986**, *110*, 421−430. (i) Gustav, K.; Storch, M. *Int. J. Quantum Chem.* **1990**, *38*, 25. (j) Grimme, S. *Chem. Phys. Lett.* **1993**, *201*, 67−74. (k) Negri, F.; Zgierski, M. Z. *J. Chem. Phys.* **1993**, *99*, 4318−4326. Eight electron CASSCF calculations with nine active orbitals. (l) Handy, N. C; Amos, R. D. Unpublished density functional theory results. (m) Kozlowski, P. M.; Rauhut, G.; Pulay, P. *J. Chem. Phys.* **1995**, *103*, 5650−5661.
(30) Brafman, O.; Chan, C. K.; Khodadoost, B.; Page, J. B.; Walker, C. T. *J. Chem. Phys.* **1984**, *80*, 5406−5417.

Table 3. CAS6+GVB/6-31G* State-Averaged Energies at Reoptimized 6-31G* geometries (Corresponding CAS6+GVB/4-31G values are in brackets)

geometry	S_0/E_h	S_1/E_h
S_1	−383.3242[a]	−383.2989[a]
	(−382.7808)	(−382.7537)
S_0/S_1	−383.2873	−383.2872
	(−382.7417)	(−382.7416)

[a] Minimum optimized with state-averaged orbitals because of CASSCF convergence difficulties.

in Figure 2 along with the CAS10 values, and the energetics are collected in Table 3 (where we also give the CAS6+GVB/4-31G energetics for comparison). Notice that, at the S_1 minimum and the S_1/S_0 conical intersection, there are two fully localized double bonds in the seven-membered ring (Scheme 1). The energy difference between the S_1/S_0 conical intersection and the S_1 minimum is 7.3 kcal mol^{-1} at the CAS6+GVB/6-31G* level (and 7.5 kcal mol^{-1} at the 4-31G level).

In conclusion, we find that the S_1 *ab initio* geometries are similar, irrespective of the level of theory (CAS6, CAS10, CAS6+GVB) used. The disagreement between *ab initio* and MMVB energy differences is associated with a local structural effect: transannular bond length compression (S_1 minimum → S_1/S_0 conical intersection) is 0.07−0.05 Å at the CASSCF level, but only 0.03 Å with MMVB; hence the barrier is larger. CASSCF is known to overestimate bond lengths, and thus geometry optimization at the CASSCF+MP2 level (when possible) would lower this barrier further. In contrast, MMVB overestimates the energies of azulene C_{2v} structures on S_0 (0−0 energy 27 kcal mol^{-1}) so that the crossing occurs slightly too early with too small a barrier. However, we believe that these results demonstrate conclusively that the existence of a low-lying conical intersection in the S_1 minimum well is a topological feature which is independent of the details of the level of theory used. In our dynamics computations, the surface hop does not generally occur at the minimum in the $n-2$ dimensional intersection space, but rather at higher energy points. Accordingly, we assume that the limited structural changes reported above will not affect the general result of the simulation.

Dynamics Simulation. Here, our objective is to study the nonequilibrium relaxation dynamics of S_1 azulene, starting from the Franck−Condon geometry S_0* and following an ensemble of trajectories that form a "classical wave packet". As reported in the computational details section, the initial conditions are determined by random sampling of each excited state normal mode within an energy threshold ΔE_{limit}.

When $\Delta E_{limit} = 0$, there is one unique reference trajectory (shown in Figure 3) where the azulene molecule starts at the Franck−Condon geometry with no excess kinetic energy. From this point, it begins to fall toward the minimum on the S_1 surface (arrows in Figure 3). During the descent, the energy separation between the S_0 and S_1 states decreases, and at the lowest point on the S_1 trajectory, it is ∼15 kcal mol^{-1}. The kinetic energy developed is sufficient to take the azulene molecule through the conical intersection where it returns to the ground state and begins to execute large amplitude vibrations. The geometry at which the surface hop occurs is shown at the top right of Figure 3 and the energy gap at this point is <1 kcal mol^{-1}. (This small energy difference at the hop is redistributed along the asymmetric nonadiabatic coupling vector, which is shown in Figure 4). Notice that the hop does not occur at the conical intersection minimum, as the geometry is distorted away from C_{2v} symmetry. However, the geometry at the hop does have the key features of the minimum energy point on the intersection

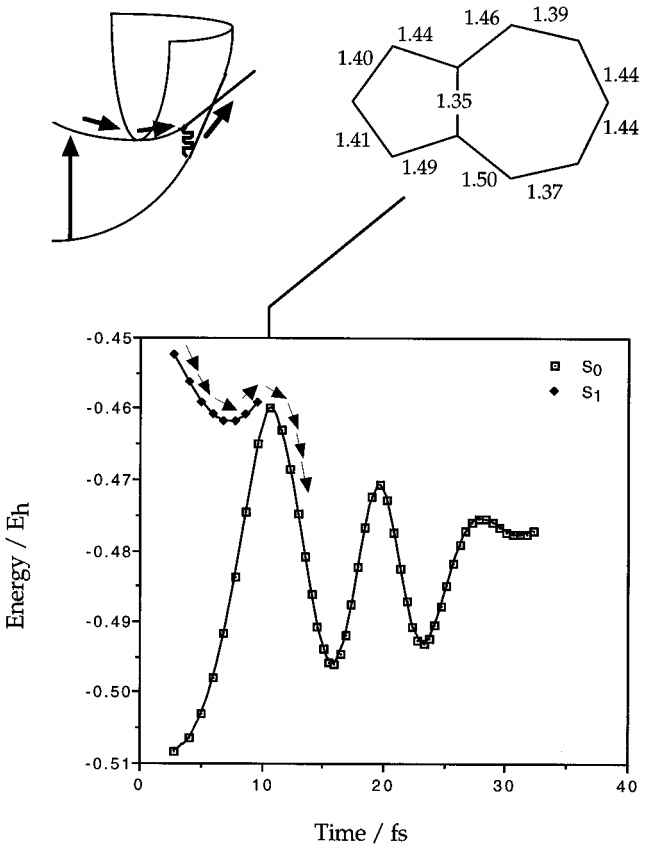

Figure 3. MMVB reference trajectory with no energy sampling ($\Delta E_{limit} = 0$). The geometry at which the $S_1 \rightarrow S_0$ surface hop takes place is shown in the top right.

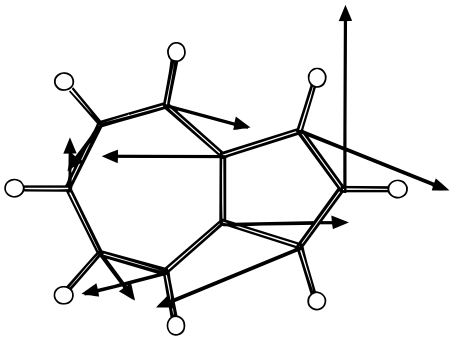

Figure 4. Nonadiabatic coupling vector computed at the CAS6 C_{2v} conical intersection minimum.

previously described, with a short transannular bond (1.35 Å) and stretched adjacent bonds within the ring. The S_1 and S_0 energy profiles along the Figure 3 trajectory reflect the S_1 relaxation coordinate discussed above: the azulene conical intersection is sloped, and accordingly, the gradients on both S_0 and S_1 are almost identical (Figure 5).

We now consider the results where the initial conditions are determined by random sampling of the excited state normal modes. The nature of this sampling is illustrated in Figure 6. The mean initial energy of the displaced starting geometries varies linearly with ΔE_{limit}. We have used vibrational excess energies which vary from 0 to ∼38 ± 10 kcal mol^{-1} on S_1, in order to sample the important regions of configuration space including the S_1 minimum and S_0/S_1 intersection.

Figure 7 illustrates one trajectory with a large (∼30 kcal mol^{-1}) vibrational excess. Contrasting with Figure 3, there are now a number of vibrations superimposed on the motion toward the minimum, which correspond to ring breathing modes. The

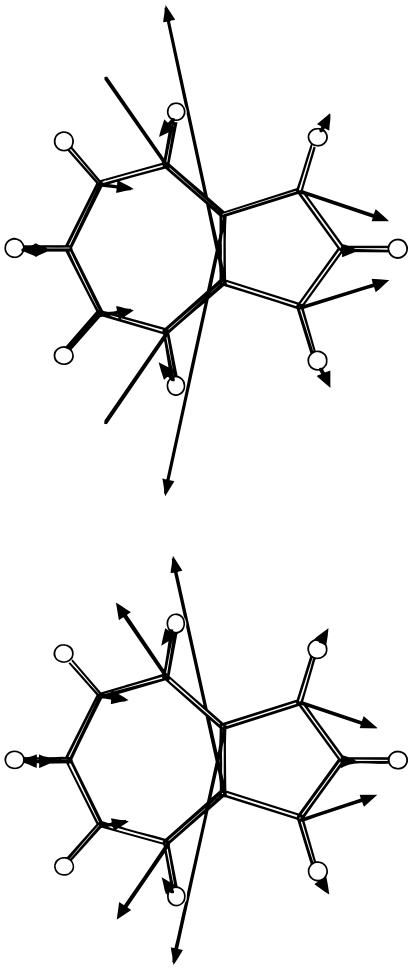

Figure 5. Gradient vectors on S_1 (top) and S_0 (bottom) at the CAS6 C_{2v} conical intersection minimum are almost identical.

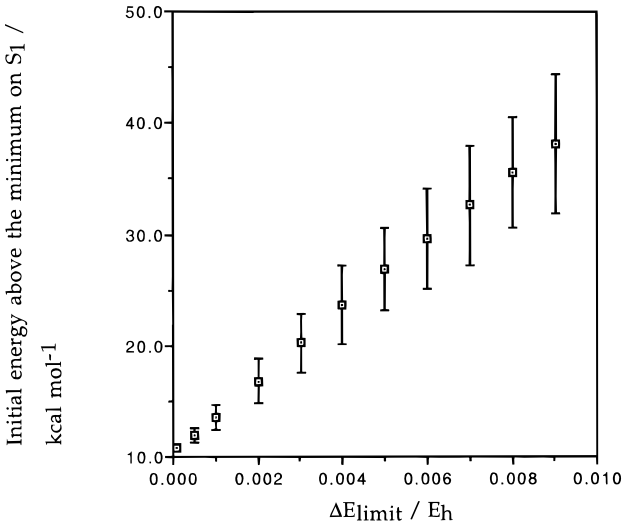

Figure 6. Energy sampling in MMVB dynamics—mean initial energy above the minimum on S_1 (kcal mol^{-1}) as a function of the input energy per mode $\Delta E_{\text{limit}}/E_{\text{h}}$. The reference geometry S_0* on S_1 is ~10 kcal mol^{-1} above the S_1 minimum.

hop geometry again has a short (1.37 Å) central bond. However, the energy gap at which the hop takes place is ~5 kcal mol^{-1}—much larger than the reference trajectory. This can be qualitatively understood in terms of the semiclassical Landau–Zener model of radiationless decay,[31] in which the probability

(31) Desouter-Lecomte, M.; Lorquet, J. C. *J. Chem. Phys.* **1977**, *71*, 4391.

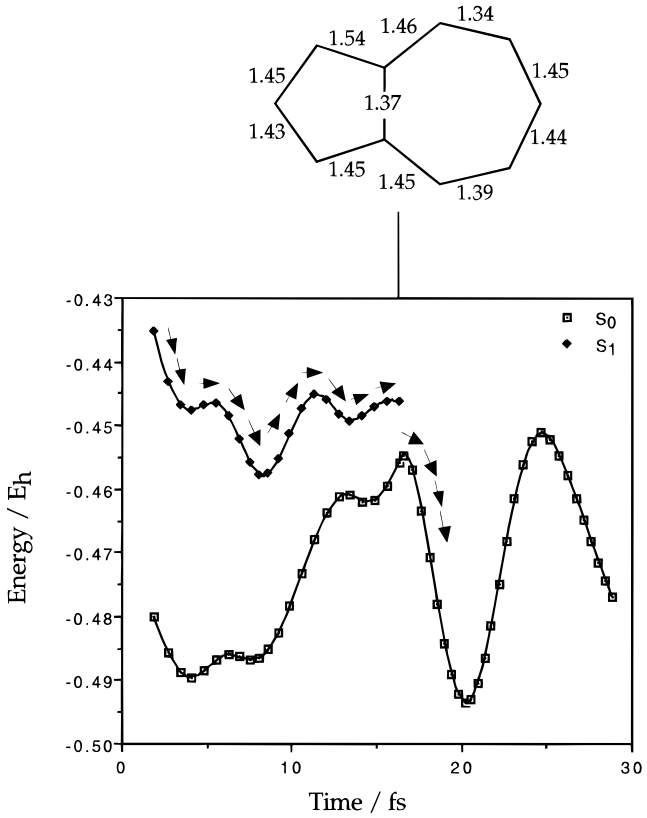

Figure 7. MMVB trajectory with energy sampling ($\Delta E_{\text{limit}} = 0.006E_{\text{h}}$). The geometry at which the surface hop takes place is shown top right.

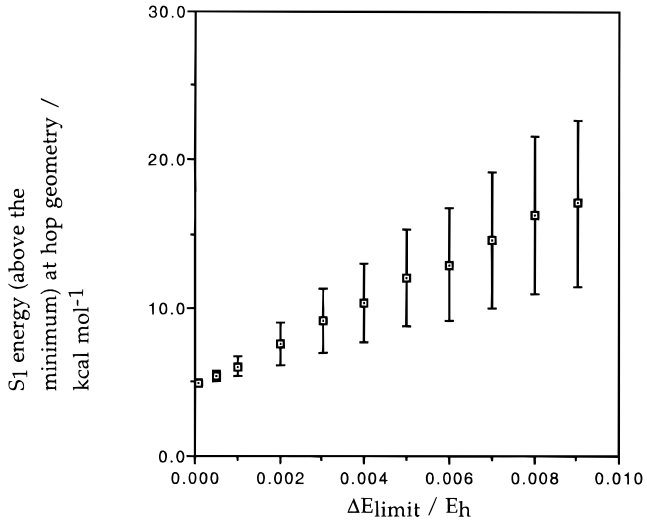

Figure 8. MMVB dynamics—mean energy of hop geometry (kcal mol^{-1}) above S_1 minimum as a function of initial energy per mode $\Delta E_{\text{limit}}/E_{\text{h}}$.

of a surface hop depends on the inverse of the kinetic energy. High kinetic energy in this case leads to a large hop gap.

All of the trajectories in our simulation led to a point on the S_0/S_1 conical intersection at which they hopped. Again, the surface hop does not, in general, occur at the minimum of the $n - 2$ dimensional crossing but rather at higher energy points. In Figure 8 we show how the energy relative to the S_1 minimum at which the hop occurs varies as a function of the initial excess vibrational energy per mode (ΔE_{limit}). With no initial kinetic energy, the hop occurs at an energy ~4 kcal mol^{-1} above the MMVB optimized conical intersection minimum (Figure 1). As the initial vibrational energy is increased, the spread of energies (error bars in Figure 8) at which the hop takes place appears to

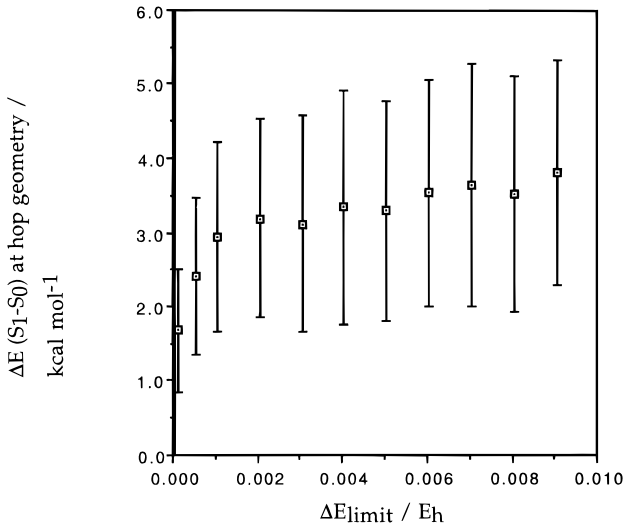

Figure 9. MMVB dynamics—mean energy difference (S_1-S_0) (kcal mol^{-1}) at the hop as a function of input energy per mode $\Delta E_{limit}/E_h$.

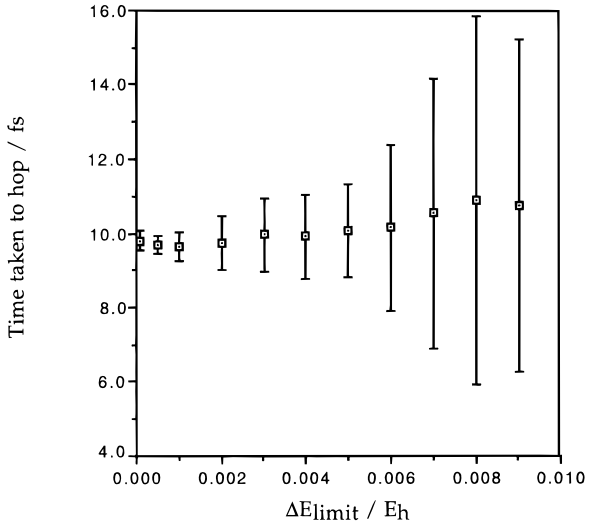

Figure 10. MMVB dynamics—mean hop time (fs) as a function of input energy per mode $\Delta E_{limit}/E_h$.

increase linearly. The range of geometries is thus quite large, and we are clearly sampling a large region of the $n - 2$ dimensional crossing. In Figure 9 we show the gap at which the hop occurs as a function of ΔE_{limit}. Remarkably, the mean value of the gap at the hop (3.5 ± 1.5 kcal mol^{-1}) is almost independent of the initial excess energy for values of $\Delta E_{limit} > 0.002E_h$, although the dispersion is large.

Figure 10 shows that the time taken to reach the surface hopping region is always ~10 fs, and it is the dispersion which increases with excess energy. However, Figure 10 masks a trend not expected classically, which is illustrated in Figure 11. At low kinetic energies, nearly all of the surface hops occur within the first half vibrational period of their excited state lifetime. At higher initial energies there is a much wider spread of crossing times with two clear peaks, corresponding to hops earlier and later than those observed at lower energy. The second peak corresponds to molecules which decay after having completed the first half of a vibration along the Scheme 1 coordinate.

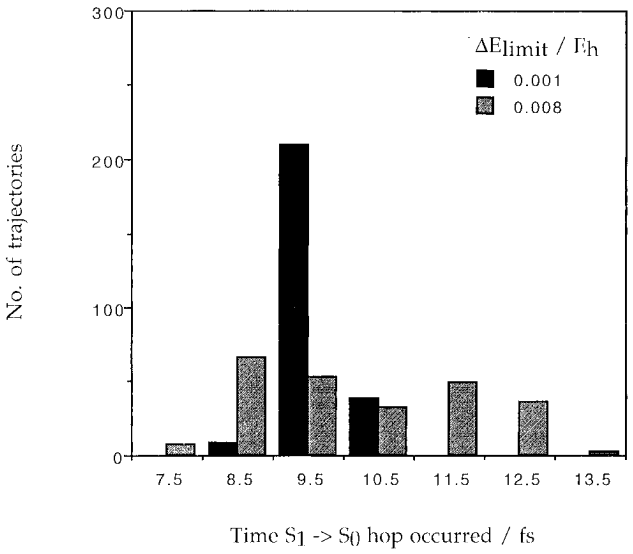

Figure 11. MMVB dynamics—hop times (fs) with small and large vibrational excesses.

The dynamics simulations presented above suggest that fast IC will approach 100% efficiency for vertically excited azulene molecules. The computed surface topology and relaxation coordinate are in complete agreement with this conclusion, suggesting that the S_1 relaxation dynamics in azulene do not depend on the accurate determination of the barrier height. As long as the Franck−Condon geometry S_0* is higher in energy than the lowest point on the S_0/S_1 intersection, a larger energy difference between the S_1 minimum and the S_1/S_0 conical intersection would merely increase the average time before a surface hop occurs.

Conclusion

CASSCF and MMVB calculations both predict the existence of a conical intersection between the S_0 and S_1 states of azulene, in agreement with the original conjecture of Longuet-Higgins.[1] Molecular dynamics simulations suggest that fast IC will approach 100% efficiency since the surface hop is seen to take place *within* one vibrational period.

In Figure 3, we show that a vibrationally cold S_1 azulene which decays to the ground state in femtoseconds and executes large amplitude initial oscillations on S_0. If the system is pumped to the S_1 state using a short (femtosecond) laser pulse, lack of even partial equilibration on the excited state means that one should be able to observe (using time-resolved pump−probe techniques) coherent vibrational motion in the newly formed population of ground state azulene. Such behavior has been observed in other systems, including large biological molecules.[32] However, in the case of azulene, this prediction awaits experimental confirmation.

Acknowledgment. This research has been supported in part by the SERC (U.K.) under Grant Numbers GR/J25123 and GR/H58070. All *ab initio* computations were run on an IBM RS/6000 using a development version of the Gaussian 92 program.[9] MMVB computations were run on a Cray T3D at the Parallel Computing Centre, University of Edinburgh (EPCC).

JA9514555

(32) Schoenlein, R. W.; Peteanu, L. A.; Mathies, R. A.; Shank, C. V. *Science* **1991**, *254*, 412.